Supporting Information

for

Self-Powered WO_3-Based Photoelectrochemical Synapse for Object Distance Judgment

Jinhai Yang, Xueqi Chen, Shengqi Huang, Xiaotian Han, Zongyu Huang, Yang Chen*, Xiang Qi*

Hunan Key Laboratory of Micro-Nano Energy Materials and Devices, School of Physics and Optoelectronics, Xiangtan University, Xiangtan, Hunan 411105, P. R. China

E-mail address: cy@xtu.edu.cn; xqi@xtu.edu.cn

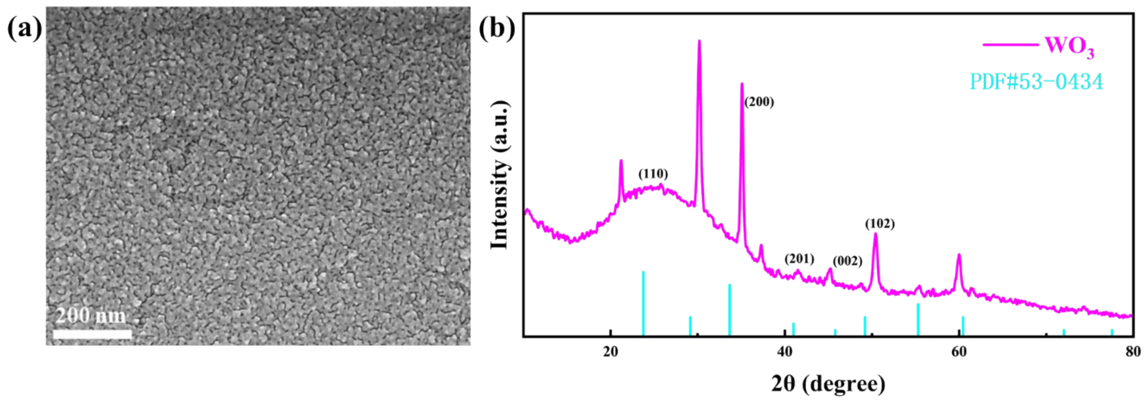

Figure S1. (a) High-magnification scanning electron microscopy (SEM) image showing detailed particle boundaries, inter-grain connections, and nanoscale surface morphologies of the WO_3 film; (b) X-ray diffraction (XRD) pattern of the prepared WO_3 film (light red curve) and standard XRD card (PDF#53-0434, wathet curve) for monoclinic WO_3, with characteristic diffraction peaks labeled as (110), (102), (200), (201), and (002). The scale bar in (a) is 200 nm; XRD test range: 20–80° (2θ).

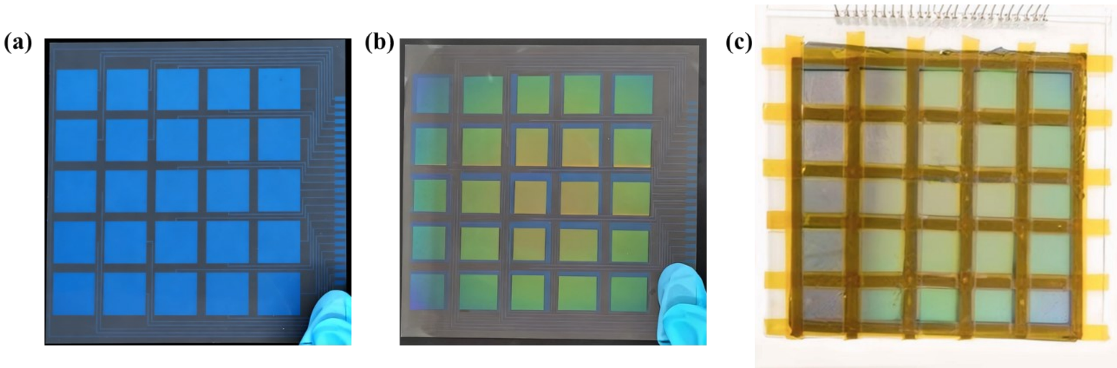

Figure S2. (a) Bare 5 × 5 array substrate (ITO glass); (b) Substrate after radio frequency (RF) sputtering of WO_3 film; (c) Schematic diagram of the WO_3-based PEC synapse device.

Key parameters: Each photoelectrode pixel has an effective area of 1.5 × 1.5 cm^2; each pixel is connected to an independent ITO wire as the photoanode; a quasi-solid electrolyte (polyvinyl alcohol-Na_2SO_4 composite) is used as the ion transport medium; conductive graphite sheets serve as the common cathode. Sputtering conditions: WO_3 target power 50 W, sputtering pressure 3 Pa, substrate temperature 0 °C, sputtering time 30 min.

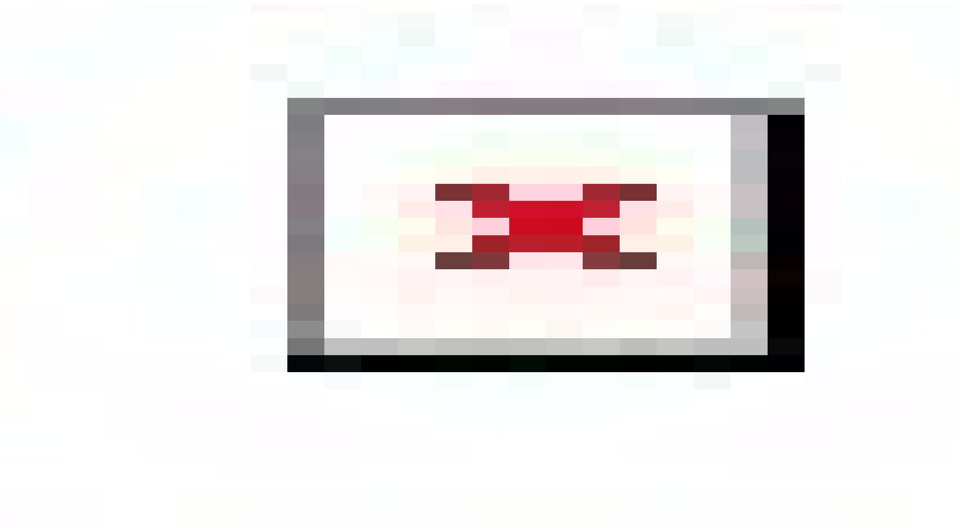

Figure S3. ΔPSV response curves of six randomly selected pixels (distributed at the center, edge, and corner of the array) to the same light pulse stimulus (light power density 120 mW/cm^2, pulse duration 10 s). The consistent response amplitude and waveform of the six pixels demonstrate good uniformity and reproducibility of the synaptic array.

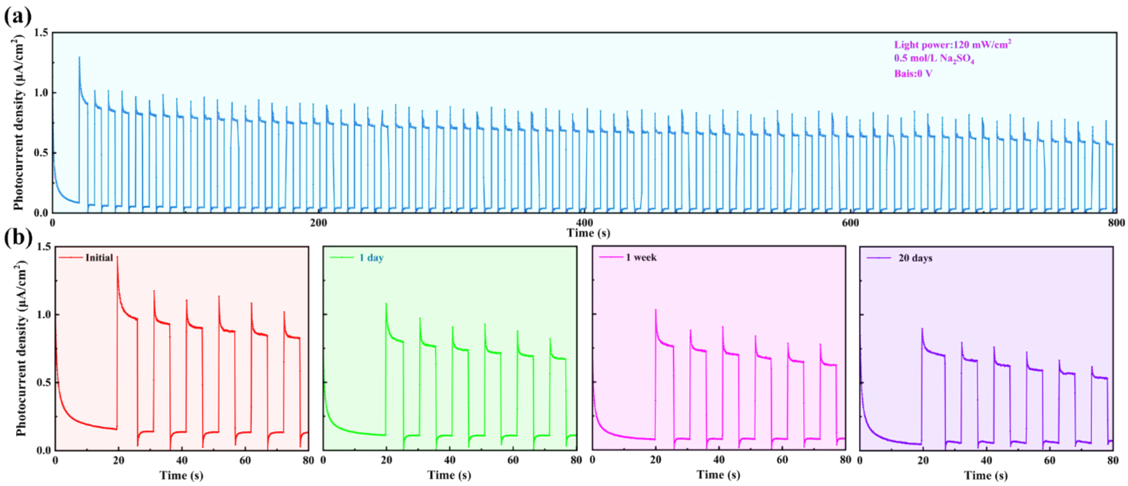

Figure S4. (a) Cycle stability: I-T response curves of the synapse device under 78 consecutive light pulse cycles (test conditions: light power 120 mW/cm^2, electrolyte 0.5 mol/L Na_2SO_4, bias 0 V); (b) Time stability: I-T response curves tested immediately after device fabrication (initial), 1 day, 1 week, and 20 days of storage (ambient temperature, dry environment, same test conditions as (a)). The stable response amplitude confirms the long-term reliability of the device.

Table S1. Raw data of distance (D), inverse square of distance ($1/D^2$), and average synaptic photovoltage (V_{avg}).

Actual Distance D(dm)	$1/D^2(dm^{-2})$	Average Synaptic Voltage V_{avg}(mV)
1	1.000	8.0±0.3
2	0.250	3.4±0.2
4	0.0625	3.0±0.2
6	0.0278	2.5±0.2
8	0.015625	1.8±0.1
10	0.0100	1.0±0.1

Note: Vavg is the average value of ΔPSV responses from 25 pixels in the 5 × 5 array, with ± values representing the standard deviation of three parallel tests; test conditions: light power 120 mW/cm² (fixed at each distance).

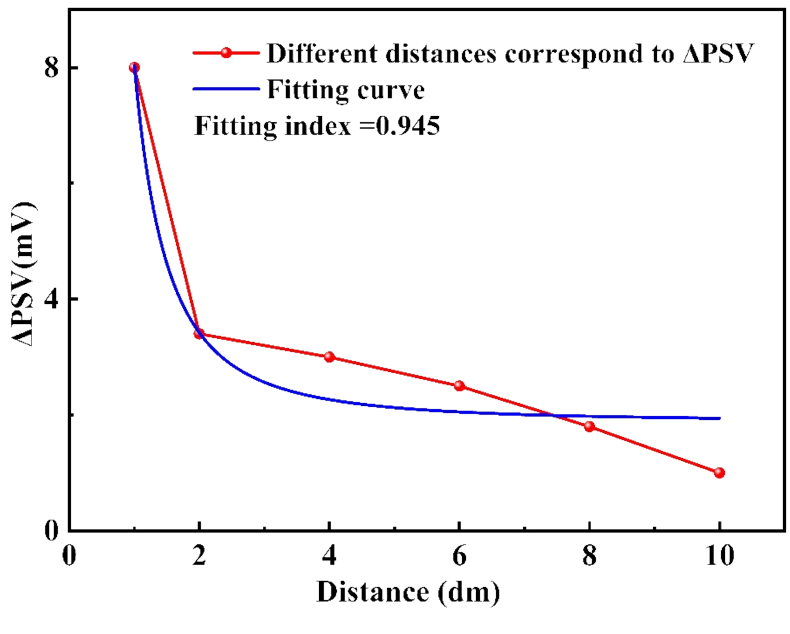

Figure S5. Scatter plot of ΔPSV (mV) versus object distance D (dm) (red dots), and the fitting curve (blue line) based on the inverse square law. Fitting equation: $\Delta PSV = 6.15\times(1/D^2) + 1.88$ ($R^2 = 0.945$). The high fitting coefficient confirms that the ΔPSV response of the synapse device follows the inverse square law of light intensity, supporting the feasibility of object distance judgment.